Heliyon 9 (2023) e21998

Contents lists available at ScienceDirect

Heliyon

journal homepage: www.cell.com/heliyon

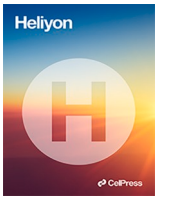

Analytical expression for the model that describes the heterogeneous reaction-diffusion process with immobilized enzyme (penicillin G acylase)

L. Niyaz Ahmed , Praveen Thomas *

Department of Mathematics, School of Advanced Sciences, Vellore Institute of Technology, Vellore, 632 014, Tamil Nadu, India

ARTICLE INFO

Keywords:
Enzyme catalyst
Modified adomian decomposition method
Akbari-ganji's method
Immobilized enzyme
Penicillin G acylase
Diffusional restrictions
Effectiveness factor

ABSTRACT

This research article examines the reaction-diffusion process in an immobilized enzyme batch reactor. The model incorporates strongly non-linear factors that are associated with standard Michaelis-Menten kinetics. The non-linear reaction-diffusion equations for substrate and product concentrations have been approximated analytically. Employing two different semi-analytical methods, Akbari-Ganji's method (AGM) and the modified Adomian decomposition method (MADM), to compute the dimensionless steady-state solutions to the system of non-linear differential equations for all values of reaction parameters. In addition, the dynamics of the mean integrated effectiveness factor of penicillin acylase in porous spherical particles have been presented for the determination of the local effectiveness factor. In order to gauge the potency of our proposed solution, we compare two semi-analytical results with a numerical result that are in good agreement across the whole concentration range. The proposed formulation aims to simulate the dynamic performance of the system utilizing the parameters and would enhance the determination of the optimum particle size for enzyme catalysts.

1. Introduction

Several factors, including pH, temperature, enzyme concentration, and substrate concentration, can influence enzyme activity. An enzyme's activity is measured by the amount of enzyme required to convert a fixed amount of substrate into a product. It can be measured by the initial phase of its progress curve [1]. Fermentation is a potential method for mass-producing enzymes for use in industry. Enzymes are synthesized via fermentation, which employs microorganisms like yeast and bacteria. Enzymes can be produced using either of two distinct fermentation processes. Submerged fermentation and fermentation on solid surfaces are two examples. Enzymes produced by microorganisms are widely used in many different industries. Enzymes from microorganisms can be genetically modified, making them a potential low-cost alternative to enzymes from plants and animals. Growing bacteria, mould, and yeast is an integral part of the fermentation process used to create microbial enzymes [2].

The significance of biological catalysis in the framework of sustainable chemical manufacturing is raised, as is the demand for enzyme immobilization as a crucial facilitating technology and for large-scale processing. Immobilization is necessary for boosting the stability and recyclability of the biocatalyst in comparison to free enzyme. The immobilization used is further impacted by the reactor configuration, such as stirred tank, fixed bed, and fluidized bed [3]. Immobilization is usually the key to boosting an enzyme's

* Corresponding author.
E-mail addresses: niyazahmed903@gmail.com (L. Niyaz Ahmed), t.praveen.vit@gmail.com, praveen.t@vit.ac.in (P. Thomas).

https://doi.org/10.1016/j.heliyon.2023.e21998
Received 11 August 2023; Received in revised form 21 October 2023; Accepted 1 November 2023
Available online 8 November 2023

operational performance in industrial processes, particularly for use in non-aqueous media [4]. Enzyme immobilization techniques are often categorized into two distinct forms based on the technique by which the chemical process is bound through support binding or entrapment. To achieve stable attachment, covalent bonds must be formed, typically through reactions involving functional groups on the protein surface. Like non-covalent adsorption, these methods can be applied to unmodified proteins [5]. The process of immobilizing Penaeus merguiensis alkaline phosphatase (PM ALP) onto gold nanorods (GNRs) was achieved through the use of ionic exchange and hydrophobic contacts. The optimal pH and temperature for achieving maximal enzyme activity in the immobilized PM ALP have been determined to be 11.0 and 60 °C, respectively, for the hydrolysis of para-Nitrophenylphosphate (p-NPP), were discussed by Homaei. A et al. [6–8]. The use of immobilized enzyme-based catalytic constructs has the potential to substantially improve a wide range of industrial processes, according to their distinct catalytic activity and reaction specificity. The enhancement of key functions in the preparation of nano-enzymes and their catalytic features will result in advantageous micro-environments for biocatalysts that are significant in industrial applications [9].

Both the bulk liquid phase, which contains the substrate (and products), and the solid enzyme catalyst phase, which is where the reaction and transformation of substrate into products take place, are modeled separately during heterogeneous enzymatic catalysis in a batch reactor. Substrate mass is moved from the bulk liquid phase into the interior of the carrier, where the enzyme is immobilized during the reaction. Fick's law and the general rate equation that characterizes enzyme catalysis are used to model the mass transfer process taking place within the catalyst particles [10].

A rate-determining step is only one of several that occur in succession in immobilized (bio) catalyst systems, particularly in porous particles. There are several steps involved in film diffusion, such as pore diffusion to the active site of the substrate molecule, bio catalytic steps (s), pore diffusion to the surface of the product molecule, and film diffusion to the bulk of the product molecule. Based on the circumstances of the reaction, each transport phase could replace the bio catalytic step as the rate-determining step. Under the current conditions, determining which step is rate-limiting is crucial [11]. In a porous catalyst, the reaction rate is regulated not only by intrinsic kinetics but also by intraparticle mass and heat transport. A reaction's efficiency is measured as the ratio of the observed rate to the rate if intraparticle mass and heat transfer resistances do not exist [12]. Penicillin acylase is a rare case of an enzyme being used effectively in the industrial manufacture of a high-value drug [13,14]. Recently, penicillin acylase has gained a lot of attention because it has expanded its role from that of a simple hydrolase in the synthesis of 6-amino penicillanic acid (6APA) from penicillin G or V to that of a valuable biocatalyst in a number of different organic synthesis reactions [15].

Immobilized enzymes undertake operations in consecutive batches, with the enzyme being retrieved after a certain point of conversion has been obtained and reused until the catalyst replacement requirement has been fulfilled [16]. Besides substrate concentration, the rate-determining variables in the rate equation are the enzyme's catalytic potential, which is in turn proportional to the enzyme's concentration and the reaction rate constant. The amount of immobilized enzyme and the amount of catalyst in the reactor both influence the enzyme concentration in the reactor. The aim of the equations is to correlate the diffusion and reaction processes within the catalyst particles. For spherical enzyme catalyst particles, a flexible system of equations is derived that permits the determination of the concentration profile of substrate within the catalyst in terms of particle geometry (radius) and concentrations of substrate in the bulk liquid phase [17]. Recently, there has been a significant focus on finding the analytical solution for the case of strongly nonlinear differential equations using various analytical approaches. Exponential approaches were used by J.I. Ramos to solve the reaction diffusion equations [18]. J. He's energy balance approach [19] was used to generate approximate solutions by D. D. Ganji et al. Work on finding exact solutions to nonlinear diffusion-reaction equations, including quadratic and cubic nonlinearities, has been done by R.S. Kaushal et al. Furthermore, it is stated that analytical solutions are used to describe many physical phenomena and are very helpful in enhancing the system [20]. Analytical solutions for Cauchy reaction-diffusion problems have been obtained by M.S.H. Chowdhury and I. Hashim by HPM; they compared HPM's efficiency to that of ADM and HAM in a study published in Ref. [21]. We present in this article a semi-analytic method for solving nonlinear differential equations, both individually and in sets, which enables the quick and simple determination of the final solution of each differential equation in the form of an algebraic function. By choosing an answer function for a differential equation with constant coefficients that can be calculated by using particular initial or boundary conditions, Akbari-Ganji's method (AGM) aims to solve all nonlinear differential equations algebraically [22]. In the steady-state regime, no rigorous analytical solution to the reaction-diffusion equations has yet been presented for the concentration of substances. Using a modified Adomian decomposition method (MADM) and Akbari-Ganji's method (AGM), we obtained an analytical expression for dimensionless substrate and product concentration. Several diffusional constraints are shown, and their corresponding dynamics are described. In addition, a range of parameter values has been analyzed to determine the evolution of the mean integrated effectiveness factor response. Error analysis of expressions for substrate concentrations and effectiveness factor response by T. Praveen et al. Performance calculations have also been done for batch reactors [23].

The key objective of this work is to validate a reaction-diffusion model by comparing the numerical solution to two solutions (the AGM and the MADM). We employed both the AGM and the MADM to compute the mean integrated effectiveness factor, with the AGM approach favouring ease of calculation. When comparing the AGM result to the numerical result, the present model's graphical depiction is more consistent with the AGM results than the MADM's approach.

2. Formulation of the problem

The modeling of reaction-diffusion phenomena within immobilized enzyme catalysts considers a uniform catalyst particle size and a uniform enzyme distribution. The equations involve substrate and product concentrations, the catalytic potential of the enzyme, which depends on the enzyme concentration, and the reaction rate constant. The equations are modeled to understand the process of diffusion and reaction inside the catalyst particles, the diffusion and reaction phenomena inside the catalyst particles are modeled to

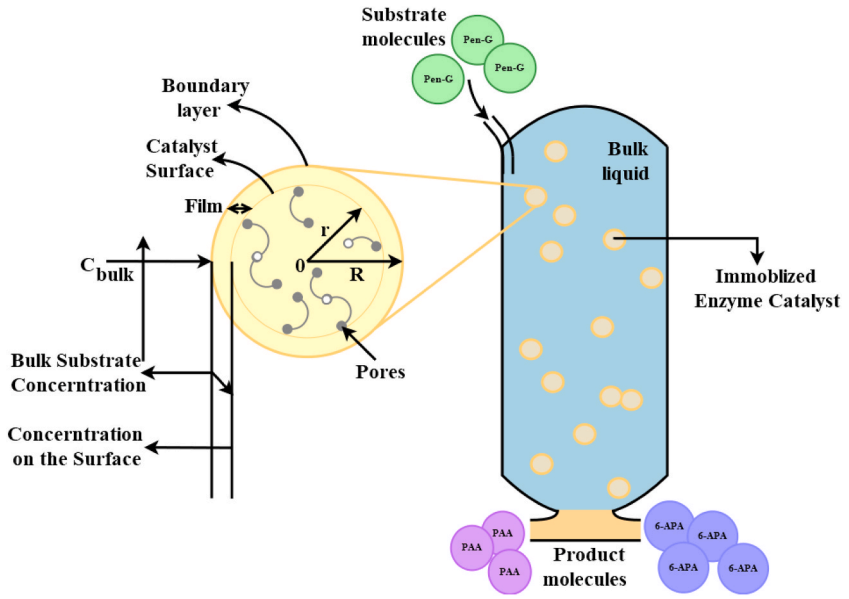

Fig. 1. Graphical representation of immobilized enzyme on a spherical catalyst particles.

understand the dynamics of reaction-diffusion. The heterogeneous nature of catalysis causes substrate and product concentration profiles inside the catalyst particle. Reaction time (t) and radial distance within the enzyme catalyst particle (r) are the variables to be considered for modeling. Now, considering a steady-state regime, time is no longer a variable, and the concentration profiles are plotted against the radial distance in Fig. 1.

The model equations have been developed with the diffusion and reaction components. The diffusion component was modeled with Fick's law, and the kinetic component was modeled considering uncompetitive inhibition by penicillin G (Pen-G), competitive inhibition by phenyl acetic acid (PAA), and non-competitive inhibition by 6-aminopenicillanic acid (6-APA) [17], [23–24]. This hypothesis is formulated on the premise that greater the volume of immobilization, the more will be overall efficacy of the result obtained using Pen-G. The chemical structure of the reactant Pen-G hydrolysis gives the product 1 as PAA and product 2 as 6-APA, as depicted in the following mechanism.

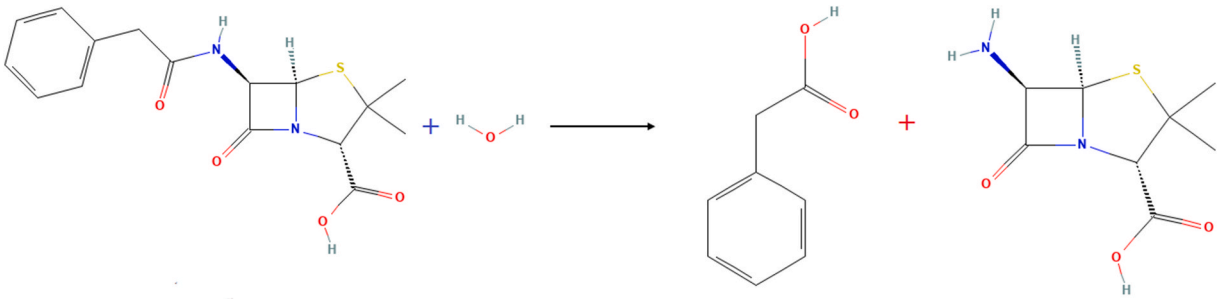

Penicillin G [Substrate (S)] PAA (P_1) 6 - APA (P_2)

The governing reaction diffusion equations are as follows [17,24]:

$$\frac{\partial S}{\partial t} = D_e\left(\frac{\partial^2 S}{\partial r^2} + \frac{2}{r}\frac{\partial S}{\partial r}\right) - v \tag{1}$$

$$\frac{\partial P_1}{\partial t} = D_{e1}\left(\frac{\partial^2 P_1}{\partial r^2} + \frac{2}{r}\frac{\partial P_1}{\partial r}\right) + v \tag{2}$$

$$\frac{\partial P_2}{\partial t} = D_{e2}\left(\frac{\partial^2 P_2}{\partial r^2} + \frac{2}{r}\frac{\partial P_2}{\partial r}\right) + v \tag{3}$$

$$v = \frac{kES}{K\left[1 + (S/K) + \left(S^2/KK_S\right) + (P_1/K_1) + (P_2/K_2) + (SP_2/KK_2) + (P_1/K_1)(P_2/K_2)\right]} \tag{4}$$

Where S is the Pen-G concentration inside biocatalyst, P_1 is the PAA concentration, P_2 is the 6-APA concentration, k the reaction rate constant, E the enzyme concentration inside the catalyst, K substrate Michaelis constant, K_S is the Pen-G inhibition constant, K_1 and K_2 are PAA, and 6-APA inhibition constants respectively, r is the radius inside the biocatalyst particle, D_e, D_{e1}, D_{e2} are the effective diffusion coefficients for Pen-G, PAA, and 6-APA respectively. Substrate diffusion occurs inside the catalyst particles in the liquid-filled cavities of the pores. This complex interaction is modeled by considering an overall diffusion process, which is controlled by a coefficient D_e, known as the effective diffusion coefficient, which considers the porous shape of the support were discussed by Valencia P et al. [17,25]. A property of both the solute and the solvent, D_e can be experimentally determined [26]. The values for the parameters involved in the equations (1)–(4) are listed in Table 9 [17,24].

In order to study a reaction-diffusion model, the following assumptions are made:

i) There is no concentration dependent interaction between the support and reactants (constant diffusivity); ii) isothermal conditions are present during reaction; iii) reactants are transported through the porous support by diffusion according to Fick's law; iv) enzyme is uniformly distributed inside catalyst particle; and v) there is no external diffusional restrictions.

The initial and boundary conditions for the equations (1)–(3) are as follows:
The initial concentrations of substrate and both products inside the catalyst particle are:

$$S(r,0) = S_{b0} \tag{5}$$

$$P_i(r,0) = 0, i = 1,2 \tag{6}$$

The boundary condition for substrate and both products concentration on a spherical particle at $r = 0$ are:

$$\frac{\partial S}{\partial r}(0,t) = 0 \tag{7}$$

$$\frac{\partial P_i}{\partial r}(0,t) = 0, i = 1,2 \tag{8}$$

This condition reflects that there is no substrate nor products flux through the center of the sphere. For all $t > 0$, concentration at the catalyst surface ($r = R$) is:

$$S(R,t) = S_b \tag{9}$$

$$P_i(R,t) = P_{bi}, i = 1,2 \tag{10}$$

The above system of equations can be converted into the dimensionless form by defining the following variables:

$$\begin{aligned} &\Phi_1 = R\sqrt{\frac{k\cdot E}{K\cdot D_e}},\ \Phi_2 = R\sqrt{\frac{k\cdot E}{K_1\cdot D_{e1}}},\ \Phi_3 = R\sqrt{\frac{k\cdot E}{K_2\cdot D_{e2}}},\ \alpha = \frac{K}{K_S},\ \beta_b = \frac{S_b}{K},\\ &\gamma_{1b} = \frac{P_{b1}}{K_1},\ \gamma_{2b} = \frac{P_{b2}}{K_2},\ \beta = \frac{S}{K},\ \gamma_1 = \frac{P_1}{K_1},\ \gamma_2 = \frac{P_2}{K_2},\ x = \frac{r}{R} \end{aligned} \tag{11}$$

Here the typical dimensionless concentration are denoted as β, γ_1 and γ_2 for S, P_1 and P_2 respectively. x is the dimensionless radial distance, Φ_1, Φ_2 and Φ_3 are the Thiele modulie. The dimensionless form of the equations (1)–(3) for the steady-state condition is as follows:

$$\frac{d^2\beta}{dx^2} + \frac{2}{x}\frac{d\beta}{dx} = \Phi_1^2 N \tag{12}$$

$$\frac{d^2\gamma_1}{dx^2} + \frac{2}{x}\frac{d\gamma_1}{dx} = -\Phi_2^2 N \tag{13}$$

$$\frac{d^2\gamma_2}{dx^2} + \frac{2}{x}\frac{d\gamma_2}{dx} = -\Phi_3^2 N \tag{14}$$

where

$$N = \frac{\beta}{1 + \beta + \alpha\beta^2 + \gamma_1 + \gamma_2 + \beta\gamma_2 + \gamma_1\gamma_2}. \tag{15}$$

The boundary conditions for the system of non-dimensional equations (12)–(14) are as follows:

$$\frac{d\beta}{dx} = \frac{d\gamma_1}{dx} = \frac{d\gamma_2}{dx} = 0; \quad \text{when} \quad x = 0 \tag{16}$$

$$\beta = \beta_b,\ \gamma_1 = \gamma_{1b},\ \gamma_2 = \gamma_{2b};\ \text{when}\ \ x = 1 \tag{17}$$

The relation between β, γ_1 and β, γ_2 are as follows

$$\beta = \frac{\Phi_1^2}{\Phi_j^2}(\gamma_{ib} - \gamma_i) + \beta_b,\ \text{where}\ \ i = 1, 2\ \text{and}\ \ j = i + 1 \tag{18}$$

Using Eq. (18), the relation among β, γ_1 and γ_2 is obtained in Eq. (19)

$$\frac{2\beta}{\Phi_1^2} + \frac{\gamma_1}{\Phi_2^2} + \frac{\gamma_2}{\Phi_3^2} = \frac{2\beta_b}{\Phi_1^2} + \frac{\gamma_{1b}}{\Phi_2^2} + \frac{\gamma_{2b}}{\Phi_3^2} \tag{19}$$

3. Materials and methods

In recent years, it has become a major research focus to develop approximate analytical methods for the reaction diffusion equations to solve nonlinear partial differential equations that are both simple and accurate. These methods include He's variation iteration method [27], Akbari-Ganji's method [22], homotopy perturbation method [28], Adomian decomposition method [29–32], modified Adomian decomposition method [33], homotopy analysis method [34], new improved generalized decomposition method [35], Duan-Rach modified Adomian decomposition method [36–38], as well as numerical techniques like the boundary element method [39], finite difference method [40], and finite element method [41]. The most significant advantage of choosing Akbar-i-Ganji's method and the modified Adomain decomposition method compared to other analytical methods is that they diminish the level of difficulty in solving nonlinear differential equations.

3.1. Akbari Ganji's method and its advantages

Catalysts are commonly employed in mass transfer chemical reactions to control the reaction rate. The catalyst's form and physical characteristics are crucial parameters in determining the differential equation that governs the chemical system. A powerful algebraic approach, Akbari-Ganji's method [22] provides semi-analytic approximation solutions to nonlinear differential equations, as mentioned in the introduction. Solutions are given in the form of convergent series, and linearization is not necessary in this method.

3.1.1. Analytical expression of dimensionless concentration of substrate and products under steady state condition using Akbari Ganji's method

In this paper, the Akbari-Ganji's method (see Appendix A) is used to solve the system of non-linear differential equations. The closed form of analytical expression of dimensionless concentrations (see Appendix B) of substrate $\beta(x)$ and products $\gamma_1(x)$ and $\gamma_2(x)$ are

$$\beta(x) = \frac{\beta_b \sinh\left(\frac{\Phi_1\ x}{\sqrt{1+\beta_b+\gamma_{1b}+\gamma_{2b}+\alpha\ \beta_b^2+\beta_b\ \gamma_{2b}+\gamma_{1b}\ \gamma_{2b}}}\right)}{x \sinh\left(\frac{\Phi_1}{\sqrt{1+\beta_b+\gamma_{1b}+\gamma_{2b}+\alpha\ \beta_b^2+\beta_b\ \gamma_{2b}+\gamma_{1b}\ \gamma_{2b}}}\right)} \tag{20}$$

Using the relation Eq. (18), the product concentrations $\gamma_1(x)$ and $\gamma_2(x)$ are obtained as follows

$$\gamma_i(x) = \gamma_{ib} - \left[\beta_b \left(\frac{\sinh\left(\frac{\Phi_1\ x}{\sqrt{1+\beta_b+\gamma_{1b}+\gamma_{2b}+\alpha\ \beta_b^2+\beta_b\ \gamma_{2b}+\gamma_{1b}\ \gamma_{2b}}}\right)}{x \sinh\left(\frac{\Phi_1}{\sqrt{1+\beta_b+\gamma_{1b}+\gamma_{2b}+\alpha\ \beta_b^2+\beta_b\ \gamma_{2b}+\gamma_{1b}\ \gamma_{2b}}}\right)} - 1\right)\right] \cdot \left[\frac{\Phi_j^2}{\Phi_1^2}\right],$$

$$\text{where}\ \ i = 1, 2\ \text{and}\ \ j = i + 1 \tag{21}$$

The Eqs. (20) and (21) satisfy the boundary conditions (16)–(17). These equations represent the new analytical expression of the concentration of substrate and products for all possible values of the parameters $\Phi_1, \Phi_2, \Phi_3, \alpha, \beta_b, \gamma_{1b}$ and γ_{2b}. The solution of γ_1 and γ_2 are same except the bulk concentration and Thiele modulus. Thus, product concentrations behave identically depending on diffusional limitations.

3.2. Modified Adomian decomposition method and its advantages

In this work, the modified Adomian decomposition method is adopted to obtain the analytical solution for the above Eqs. (12)–(14)

for the conditions (16)–(17). In recent years, many authors handled MADM to solve strongly non-linear problems. MADM provides more realistic series solutions that generally converge very rapidly in real physical problems. The rapid convergence shows that this method is reliable [33,37]. The constructive procedure and choice of handling the operator are provided by M. M. Hosseini and M. Jafari [42,43]. The decomposition method is straightforward, without restrictive assumptions, and the components of the series solution can be easily computed using any mathematical symbolic package [44].

3.2.1. Solution of dimensionless concentration of substrate and products under steady state condition using modified Adomian decomposition method

We have also employed the modified Adomian decomposition method (see Appendix C) to solve the system of non-linear differential equations. The simple and closed form of analytical expression of dimensionless concentrations (see Appendix D) of substrate $\beta(x)$ and products $\gamma_1(x)$ and $\gamma_2(x)$ are

$$\beta(x) = \beta_b + A \cdot \left[\Phi_1^2\left(x^2 - 1\right)\right] \tag{22}$$

$$A = \frac{1}{6}\left[\frac{\beta_b}{1 + \beta_b + \alpha\beta_b^2 + \gamma_{1b} + \gamma_{2b} + \gamma_{2b}\beta_b + \gamma_{1b}\gamma_{2b}}\right] \tag{23}$$

Using the relation Eq. (18), the product concentrations $\gamma_1(x)$ and $\gamma_2(x)$ are obtained as follows

$$\gamma_i(x) = \gamma_{ib} - [\beta(x) - \beta_b] \cdot \left[\frac{\Phi_j^2}{\Phi_1^2}\right], \quad \text{where } i = 1, 2 \text{ and } j = i + 1 \tag{24}$$

The Eqs. (22)–(24) satisfy the boundary conditions (16)–(17). These equations represent the new analytical expression of the concentration of substrate and products for all possible values of the parameters $\Phi_1, \Phi_2, \Phi_3, \alpha, \beta_b, \gamma_{1b}$ and γ_{2b}. The solution of γ_1 and γ_2 are same except the bulk concentration and Thiele modulus. Therefore behaviors of the both product concentrations are almost same, varies with the diffusional restrictions.

3.2.2. Solution with degree of conversion

Consider a degree of conversion for the concentration of substrate and products respectively as,

$$X = \frac{\beta_{b0} - \beta_b}{\beta_{b0}}; X = \frac{P_{1b}}{S_{b0}} = \frac{P_{2b}}{S_{b0}} = \frac{\gamma_{1b}K_1}{\beta_{b0}K} = \frac{\gamma_{2b}K_2}{\beta_{b0}K} \tag{25}$$

Bulk concentrations in function of degree of conversion:

$$\beta_b = \beta_{b0}(1 - X);\ \gamma_{1b} = \frac{\beta_{b0}K}{K_1}X;\ \text{and}\ \ \gamma_{2b} = \frac{\beta_{b0}K}{K_2}X \tag{26}$$

Replacing in Eqs. (20) and (22), we get the concentrations inside catalyst as

$$\beta(x) = \beta_{b0}(1 - X) + A\Phi_1^2\left(x^2 - 1\right) \tag{27}$$

$$\gamma_1(x) = \frac{\beta_{b0}K}{K_1}X + A\Phi_2^2\left(1 - x^2\right) \tag{28}$$

$$\gamma_2(x) = \frac{\beta_{b0}K}{K_2}X + A\Phi_3^2\left(1 - x^2\right) \tag{29}$$

$$A = \frac{1}{6}\left[\frac{\beta_{b0}(1 - X)}{1 + \beta_{b0}(1 - X) + \alpha[\beta_{b0}(1 - X)]^2 + \frac{\beta_{b0}K}{K_1}X + \frac{\beta_{b0}K}{K_2}X + \frac{\beta_{b0}K}{K_2}X\beta_{b0}(1 - X) + \frac{\beta_{b0}K}{K_1}X\frac{\beta_{b0}K}{K_2}X}\right] \tag{30}$$

The limitation of the proposed solution for substrate concentration $\beta(x)$ is given as follows by the following constrain:

$$6\begin{pmatrix} K_1K_2 + \beta_{b0}(1 - X)K_1K_2 + \alpha\beta_{b0}^2(1 - X)^2K_1K_2 + \\ \beta_{b0}XKK_2 + \beta_{b0}XKK_1 + \beta_{b0}X(1 - X)KK_1 + \beta_{b0}^2X^2K^2 \end{pmatrix} - \Phi_1^2K_1K_2 > 0 \tag{31}$$

Based on the combination of β_{b0} and Φ_1 as determined by Eq. (31), Fig. 9(a and b) illustrates the acceptable and unacceptable areas of the proposed solution. The white zone denotes the valid solution region, while the red zone denotes the invalid solution region.

4. The global integral effectiveness factor is as follows

From the present study, we can investigate the effectiveness of a catalyst or reactor in promoting a chemical reaction, considering

the influence of reaction kinetics and mass transport (diffusion) within the system. Additionally, it assesses the efficiency of substrate transportation to the catalyst and the removal of products from it. The usage of this technique facilitates the optimization of reaction speeds while simultaneously minimizing the occurrence of inefficient side reactions. Its value can be used to determine the potential of a particular reactor or catalyst for performing the intended chemical conversion. For a spherical catalyst particle, the global integral effectiveness factor is [45].

$$\eta' = 3\int_0^1 \eta \cdot x^2 \cdot dx \tag{32}$$

The local effectiveness factor depends on the reaction rate equation. The general definition is:

$$\eta = \frac{\text{reaction rate inside catalyst}}{\text{reaction rate at catalyst surface}} = \frac{v(S(r),P(r))}{v(S_b,P_b)} \quad \text{conditions}\left(\begin{matrix}\text{bulk}\\ \text{conditions}\end{matrix}\right) \tag{33}$$

For the penicillin acylase reaction-diffusion equation, the local effectiveness factor is obtained by replacing N in the above definition.

$$\eta = \frac{\beta\left(1+\beta_b+\alpha{\beta_b}^2+\gamma_{1b}+\gamma_{2b}+\gamma_{2b}\beta_b+\gamma_{1b}\gamma_{2b}\right)}{\beta_b\left(1+\beta+\alpha\beta^2+\gamma_1+\gamma_2+\gamma_2\beta+\gamma_1\gamma_2\right)} \tag{34}$$

4.1. Mean integrated effectiveness factor for the concentration of substrate using AGM solution

The mean integrated effectiveness factor obtained using Eqs. (32) and (34) is as follows:

$$\eta' = \left(\frac{3}{\Lambda^2}\right)[\Lambda\coth(\Lambda)-1], \text{where } \Lambda = \frac{\Phi_1}{\sqrt{1+\beta_b+\gamma_{1b}+\gamma_{2b}+\alpha\,\beta_b^2+\gamma_{2b}\,\beta_b+\gamma_{1b}\,\gamma_{1b}}} \tag{35}$$

The dynamics of the mean integrated effectiveness factor is provided in the Table 7(a - d).

4.2. Mean integrated effectiveness factor for the concentration of substrate using MADM solution

The mean integrated effectiveness factor obtained using Eqs. (32), (34) is as follows:

$$\eta' = \frac{1}{12}\frac{\left\{\begin{array}{l}\sqrt{DE-2E^2-Q_1}\left[\begin{array}{l}\sqrt{2}\,Q_3\,A_1\,D\,E-\sqrt{2}\,Q_3\,B\,D^2+2\sqrt{2}\,Q_3\,B\,D\,E-\sqrt{2}\,Q_3\,B\,D\,\sqrt{D^2-4EC}-2\sqrt{2}\,Q_3\,E^2\,A_1\\ +2\sqrt{2}\,Q_3\,B\,E\sqrt{D^2-4EC}+2\sqrt{2}\,Q_3\,B\,C\,E+\sqrt{2}\,Q_3\,A_1\,E\sqrt{D^2-4EC}-2\sqrt{2}\,Q_3\,E^2B\end{array}\right]+\\ \sqrt{DE-2E^2+Q_1}\left[\begin{array}{l}\sqrt{2}Q_2\,B\,D^2-2\sqrt{2}\,Q_2\,B\,D\,E-\sqrt{2}\,Q_2\,B\,D\sqrt{D^2-4EC}-\sqrt{2}\,Q_2\,A_1\,D\,E+2\sqrt{2}\,Q_2\,E^2B\\ +\sqrt{2}\,Q_2\,A_1E\,\sqrt{D^2-4EC}-2\sqrt{2}Q_2\,B\,C\,E+2\sqrt{2}\,Q_2\,B\,E\sqrt{D^2-4EC}+2\sqrt{2}\,Q_2\,E^2A_1\end{array}\right]+\end{array}\right\}}{2B\sqrt{D^2-4EC}\sqrt{DE-2E^2-Q_1}\sqrt{DE-2E^2+Q_1}} \tag{36}$$

where $Q_1 = E\sqrt{D^2-4EC}$; $Q_2 = \tan^{-1}\left[\frac{\sqrt{2}E}{\sqrt{D-2E-E\sqrt{D^2-4EC}}}\right]$; $Q_3 = \tan^{-1}\left[\frac{\sqrt{2}E}{\sqrt{D-2E+E\sqrt{D^2-4EC}}}\right]$; $A_1 = [18(1+\beta_b+\alpha{\beta_b}^2+\gamma_{1b}+\gamma_{2b}+\gamma_{2b}\beta_b+\gamma_{1b}\gamma_{2b})-3\Phi_1^2]$; $B = 3\Phi_1^2$; $C = (1+\beta_b+\alpha{\beta_b}^2+\gamma_{1b}+\gamma_{2b}+\gamma_{2b}\beta_b+\gamma_{1b}\gamma_{2b})$;

$$\begin{gathered} D = (M_1+2\alpha\beta_bM_1+\gamma_{2b}M_1-M_2-M_3-\beta_bM_3-M_3\gamma_{1b}-M_1\gamma_{2b});\ E = \left(\alpha M_1^2+M_2M_3-M_1M_3\right);\\ M_i = \frac{\Phi_i^2\beta_b}{6\left(1+\beta_b+\alpha\beta_b^2+\gamma_{1b}+\gamma_{2b}+\gamma_{2b}\beta_b+\gamma_{1b}\gamma_{2b}\right)};\ i=1,2,3;\\ \beta_b = \beta_{b0}(1-X);\ \gamma_{1b} = \frac{\beta_{b0}K}{K_1}X;\ \text{and}\ \ \gamma_{2b} = \frac{\beta_{b0}K}{K_2}X \end{gathered} \tag{37}$$

when comparing the MADM with the AGM for calculating the mean integrated effectiveness factor, the AGM provides a simpler computation, whereas the MADM gives a more comprehensive mathematical expression. The dynamics of the mean integrated effectiveness factor is provided in the Table 8(a - c).

5. Results and discussion

The concentration of substrate (Pen-G) and products (PAA, 6-APA, respectively) depends upon the Thiele modulus $\Phi_i; i = 1, 2, 3$. In addition, we analyze the behavior of graphs depicting the relationship between dimensionless substrate concentration β and product concentrations $\gamma_i; i = 1, 2$ over dimensionless radial distance x, as a function of the Thiele modulus Φ for various values of β_{b0}. The graphs based on Fig. 2(a–d), 3 (a - d), and 4 (a - d) represent the mechanisms of uncompetitive substrate inhibition by Pen-G, competitive product inhibition by PAA, and non-competitive product inhibition by 6-APA (see Tables 1 and 2).

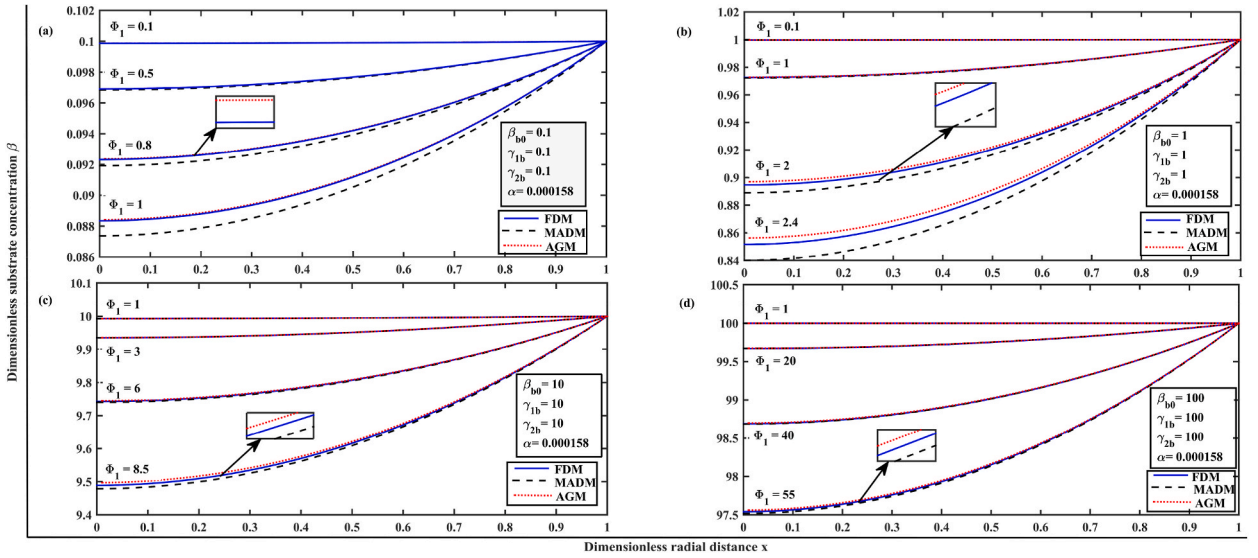

Fig. 2. Comparison of dimensionless substrate concentration β **versus dimensionless radial distance** x **with numerical simulation results (FDM) for various diffusional restrictions** Φ_1 **and different initial bulk substrate concentration** β_{b0} **(a) 0.1 (b) 1 (c) 10 and (d) 100 using Eqs. (12), (20) and (22).**

Table 1

(a) Comparison of dimensionless uncompetitive inhibition by Pen-G concentration of substrate β (Eq. (20), (22)) and numerical simulation against the dimensionless radial distance x for different values of Thiele modulus Φ_1 and ($\beta_{b0} = \gamma_{1b} = \gamma_{2b} = 100, \alpha = 0.000158$).

$\Phi_1 = 0.1$						$\Phi_1 = 1$				
X	AGM (20)	MADM (22)	Numerical (FDM)	% of Error (20)	% of Error (22)	AGM (20)	MADM (22)	Numerical (FDM)	% of Error (20)	% of Error (22)
0.0	100	100	100	0	0	99.9992	99.9991	99.9991	0.0001	0
0.2	100	100	100	0	0	99.9992	99.9992	99.9992	0	0
0.4	100	100	100	0	0	99.9993	99.9993	99.9993	0	0
0.6	100	100	100	0	0	99.9995	99.9994	99.9994	0.0001	0
0.8	100	100	100	0	0	99.9997	99.9997	99.9997	0	0
1.0	100	100	100	0	0	100	100	100	0	0
Average % of Error				0	0	Average % of Error			0.00003	0

(b)

$\Phi_1 = 5$						$\Phi_1 = 10$				
X	AGM (20)	MADM (22)	Numerical (FDM)	% of Error (20)	% of Error (22)	AGM (20)	MADM (22)	Numerical (FDM)	% of Error (20)	% of Error (22)
0.0	99.979	99.979	99.975	0.004	0.004	99.92	99.92	99.92	0	0
0.2	99.982	99.981	99.981	0.0001	0	99.92	99.92	99.92	0	0
0.4	99.983	99.983	99.983	0	0	99.93	99.93	99.93	0	0
0.6	99.987	99.987	99.987	0	0	99.95	99.95	99.95	0	0
0.8	99.994	99.994	99.994	0	0	99.97	99.97	99.97	0	0
1.0	100	100	100	0	0	100	100	100	0	0
Average % of Error				0.0007	0.0006	Average % of Error			0	0

Table 2

(a) Comparison of dimensionless uncompetitive inhibition by Pen-G concentration of substrate γ_1 (Eq. (21), (24)) and numerical simulation against the dimensionless radial distance x for different values of Thiele modulus Φ_2 and ($\beta_{b0} = \gamma_{1b} = \gamma_{2b} = 100, \Phi_1 = 0.1, \alpha = 0.000158$).

$\Phi_2 = 0.1$						$\Phi_2 = 1$				
X	AGM (20)	MADM (22)	Numerical (FDM)	% of Error (20)	% of Error (22)	AGM (20)	MADM (22)	Numerical (FDM)	% of Error (20)	% of Error (22)
0.0	100	100	100	0	0	100	100.0008	100.0008	0.0008	0
0.2	100	100	100	0	0	100	100.0008	100.0008	0.0008	0
0.4	100	100	100	0	0	100	100.0007	100.0007	0.0007	0
0.6	100	100	100	0	0	100	100.0005	100.0005	0.0005	0
0.8	100	100	100	0	0	100	100.0003	100.0003	0.0003	0
1.0	100	100	100	0	0	100	100	100	0	0
Average % of Error				0	0	Average % of Error			0.00052	0

(b)

$\Phi_2 = 5$						$\Phi_2 = 10$				
X	AGM (20)	MADM (22)	Numerical (FDM)	% of Error (20)	% of Error (22)	AGM (20)	MADM (22)	Numerical (FDM)	% of Error (20)	% of Error (22)
0.0	100	100.020	100.020	0.0199	0	100	100.08	100.08	0.0799	0
0.2	100	100.019	100.019	0.0189	0	100	100.08	100.08	0.0799	0
0.4	100	100.017	100.017	0.0169	0	100	100.07	100.07	0.0699	0
0.6	100	100.014	100.013	0.0129	0.0009	100	100.05	100.05	0.0499	0
0.8	100	100.007	100.007	0.0007	0	100	100.03	100.03	0.0299	0
1.0	100	100	100	0	0	100	100	100	0	0
Average % of Error				0.0116	0.0002	Average % of Error			0.0516	0

Table 3

Concentration of uncompetitive substrate inhibition by Pen-G β (AGM, Eq. (20)) against the dimensionless radial distance x for various values of Thiele modulus Φ_1 and (at$x = 0, \alpha = 0.000158$).

$\beta_{bo} = \gamma_{1b} = \gamma_{2b} = 0.1$		$\beta_{bo} = \gamma_{1b} = \gamma_{2b} = 1$		$\beta_{bo} = \gamma_{1b} = \gamma_{2b} = 10$		$\beta_{bo} = \gamma_{1b} = \gamma_{2b} = 100$	
Φ_1	β	Φ_1	β	Φ_1	β	Φ_1	β
0.1	0.09987	0.1	0.9997	0.1	10.000	1	100.00
0.3	0.09887	1	0.9728	1	9.993	10	99.92
0.5	0.09691	1.5	0.9401	3	9.935	20	99.67
0.8	0.09235	2	0.8970	6	9.745	40	98.70
1	0.08841	2.4	0.8563	8.5	9.497	55	97.56

Table 4

Concentration of competitive product inhibition by PAA and non-competitive product inhibition by 6-APA (γ_1, γ_2) (AGM, Eq. (21)) against the dimensionless radial distance x for various values of Thiele moduli Φ_2, Φ_3 and (at$x = 0, \alpha = 0.000158, \Phi_1 = 0.1$).

$\beta_{bo} = \gamma_{1b} = \gamma_{2b} = 0.1$		$\beta_{bo} = \gamma_{1b} = \gamma_{2b} = 1$		$\beta_{bo} = \gamma_{1b} = \gamma_{2b} = 10$		$\beta_{bo} = \gamma_{1b} = \gamma_{2b} = 100$	
Φ_2, Φ_3	γ_1, γ_2	Φ_2, Φ_3	γ_1, γ_2	Φ_2, Φ_3	γ_1, γ_2	Φ_2, Φ_3	γ_1, γ_2
0.1	0.1001	0.1	1	1	10.01	1	100
1	0.1126	1	1.028	3	10.06	25	100.5
2	0.1505	2	1.111	7	10.35	45	101.7
2.5	0.1788	3.4	1.321	10	10.72	60	103

Table 5

Concentration of uncompetitive substrate inhibition by Pen-G β (MADM, Eq. (22)) against the dimensionless radial distance x for various values of Thiele modulus Φ_1 and (at$x = 0, \alpha = 0.000158$).

$\beta_{bo} = \gamma_{1b} = \gamma_{2b} = 0.1$		$\beta_{bo} = \gamma_{1b} = \gamma_{2b} = 1$		$\beta_{bo} = \gamma_{1b} = \gamma_{2b} = 10$		$\beta_{bo} = \gamma_{1b} = \gamma_{2b} = 100$	
Φ_1	β	Φ_1	β	Φ_1	β	Φ_1	β
0.1	0.09987	0.1	0.9997	0.1	10.000	1	100.00
0.3	0.09886	1	0.9722	1	9.993	10	99.92
0.5	0.09684	1.5	0.9375	3	9.935	20	99.67
0.8	0.09192	2	0.8889	6	9.740	40	98.69
1	0.08737	2.4	0.8400	8.5	9.479	55	97.52

Table 6
Concentration of competitive product inhibition by PAA and non-competitive product inhibition by 6-APA (γ_1, γ_2) (MADM, Eq. (24)) against the dimensionless radial distance x for various values of Thiele moduli Φ_2, Φ_3 and ($at x = 0, \alpha = 0.000158, \Phi_1 = 0.1$).

$\beta_{bo} = \gamma_{1b} = \gamma_{2b} = 0.1$		$\beta_{bo} = \gamma_{1b} = \gamma_{2b} = 1$		$\beta_{bo} = \gamma_{1b} = \gamma_{2b} = 10$		$\beta_{bo} = \gamma_{1b} = \gamma_{2b} = 100$	
Φ_2, Φ_3	γ_1, γ_2	Φ_2, Φ_3	γ_1, γ_2	Φ_2, Φ_3	γ_1, γ_2	Φ_2, Φ_3	γ_1, γ_2
0.1	0.1001	0.1	1	1	10.01	1	100
1	0.1126	1	1.028	3	10.06	25	100.5
2	0.1505	2	1.111	7	10.35	45	101.7
2.5	0.1789	3.4	1.321	10	10.72	60	103

Table 7
Mean integrated effectiveness factor for uncompetitive substrate inhibition by Pen-G η' against the initial bulk concentration β_{b0} (a) 0.1 (b) 1 (c) 10 and (d) 100 using (AGM, Eq. (35)) for various values of Thiele modulus Φ_1 and ($\Phi_2 = \Phi_3 = 0.1, \alpha = 0.000158$).

$\beta_{b0} = 0.1$		$\beta_{b0} = 1$		$\beta_{b0} = 10$		$\beta_{b0} = 100$	
Φ_1	η'	Φ_1	η'	Φ_1	η'	Φ_1	η'
0.1	0.9995	0.1	0.9999	1	0.9997	1	1
0.5	0.9876	1	0.9891	3	0.9974	20	0.9987
0.8	0.9691	2	0.9582	6	0.9898	40	0.9948
1	0.9529	2.4	0.9413	8.5	0.9798	55	0.9902

Table 8
Mean integrated effectiveness factor for uncompetitive substrate inhibition by Pen-G for η' against the initial bulk concentration β_{b0} (a) 0.1 (b) 1 and (c) 10 using (MADM, Eq. (36)), for various values of Thiele modulus Φ_1 and ($\Phi_2 = \Phi_3 = 0.1, \alpha = 0.000158, X = 0, K = 0.13, K_1 = 1.82, K_2 = 48$).

$\beta_{b0} = 0.1$		$\beta_{b0} = 1$		$\beta_{b0} = 10$	
Φ_1	η'	Φ_1	η'	Φ_1	η'
0.2	0.9977	0.2	0.9988	0.2	0.9993
1	0.9475	1	0.9824	3	0.9941
2	0.8071	3.5	0.7043	6	0.9714
3.4	0.3208	4.6	0.1119	8.5	0.7545

Table 9
Kinetic and diffusional constants for penicillin G hydrolysis model [17,24].

Substance	Parameter	Value	Units
Enzyme	k	43	1/s
Penicillin G	K	0.13	mM
Penicillin G	K_s	821	mM
PAA	K_1	1.82	mM
APA	K_2	48	mM
Penicillin G	D_e	5.30×10^{-10}	m^2/s
PAA	D_{e1}	7.33×10^{-10}	m^2/s
APA	D_{e2}	5.89×10^{-10}	m^2/s

5.1. *Effect of thiele modulus* $\Phi_1 = R\sqrt{\frac{k\,E}{K\,D_e}}$ *for the concentration of uncompetitive substrate inhibition*

The concentration of substrate within the catalyst decreases in all cases (a) – (d) as the Thiele modulus increases, as depicted in Fig. 2(a–d), and shown in Tables 3 and 5. Moreover, the effectiveness factor η' will decrease in all cases, referring to Fig. 5(a–d). The observation signifies that an increase in substrate concentration in the bulk β_{b0} leads to a decrease in diffusional restriction $\left(\text{i.e.}\Phi_1 \ll 0.1 \Rightarrow \frac{\beta}{\beta_{b0}} \rightarrow 1\right)$. For all β_{b0} values with a lower Thiele modulus have the highest effectiveness factor, which is tabulated in Table 7(a - d) and 8 (a - c), i.e., $(\forall \beta_{b0}\ (\Phi_1 \ll 0.1\ \Rightarrow \eta' \rightarrow 1))$ which indicates that the catalyst is highly efficient. As diffusional restriction increases, the effectiveness factor begins to reduce. Diffusional control governs the response when the Thiele modulus is high $(\Phi_1 \gg 0.1)$. This phenomenon is observed under conditions of intense catalytic activity with minimal reaction rate constants.

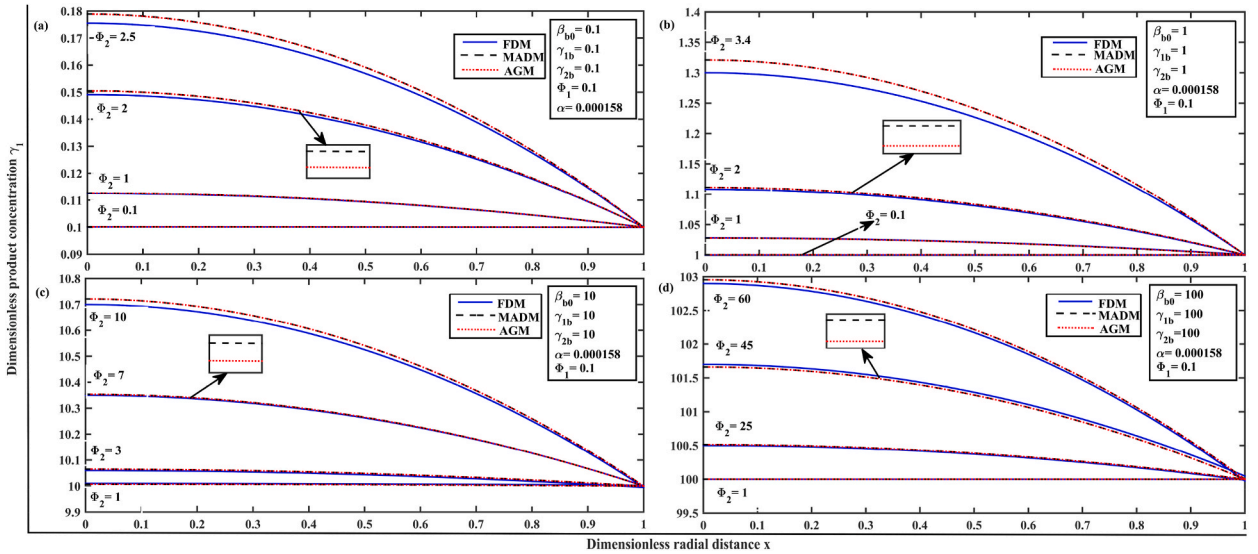

Fig. 3. Comparison of dimensionless product concentration γ_1 versus dimensionless radial distance x with numerical simulation results (FDM) for various diffusional restrictions Φ_2 and different initial bulk product concentration γ_{1b} (a) 0.1 (b) 1 (c) 10 and (d) 100 using Eq. (13), (21) and (24).

5.2. *Effect of thiele modulus* $\Phi_2 = R\sqrt{\frac{k\,E}{K_1\,D_{e_1}}}$ *for the concentration of competitive product inhibition*

As the concentration of competitive product inhibition drops, the Thiele modulus Φ_2 is also minimally driven in all cases (a)–(d), as depicted in Fig. 3(a–d), and in the Tables 4 and 6. The majorities of the reactant concentration and the Thiele modulus are predominantly influenced by the reaction kinetics and the diffusivity characteristics within the catalyst particle. As the concentration of the competitive product rises, it begins to retard the reaction by occupying the active sites on the surface of the catalyst. As a result, there is a reduction in the value of the reaction rate constant 'k', leading to an appropriate decrease in the Thiele modulus Φ_2. The inhibitory effect can be intensified by a higher Thiele modulus in the presence of competitive product inhibition. The reaction rate may be limited due to the reduced availability of the reactant at the catalyst surface, which is caused by the concentration gradient of the reactant resulting from internal diffusion resistance.

5.3. *Effect of thiele modulus* $\Phi_3 = R\sqrt{\frac{k\,E}{K_2\,D_{e_2}}}$ *for the concentration of non-competitive product inhibition*

A decrease in the Thiele modulus Φ_3 entails a maximum reaction rate relative to the diffusion rate. Given the Thiele modulus $\Phi_3 \approx 0.1(\text{or})1$, it can be inferred that the rates of reaction and diffusion are of similar magnitude. The Thiele modulus Φ_3 may have an impact on the concentration of the non-competitive product inhibitor. The concentration of the inhibitor may become monotone depending on the interplay between reaction and diffusion rate in a specific system as the Thiele modulus increases ($\Phi_3 \gg 0.1(\text{or})1$). As represented in Fig. 4(a–d), and in the Tables 4 and 6, it is apparent that an increase in Thiele modulus triggers a corresponding increase in product concentration across all cases, which leads to the diffusion rate exceeding the reaction rate.

The flexibility of the reaction-diffusion model's solution is determined by alterations in reaction and mass transfer rates. The two phenomena are impacted by two common factors, which are the bulk substrate concentration β_{b0} and the Thiele modulus $\Phi_i; i = 1, 2, 3$. The reaction rate of each analyzed mechanism is influenced by the substrate concentration. The impact is prominent until the concentration of $\beta_{b0} = 10$, at which point the enzyme becomes saturated with substrate and the reaction rate no longer exhibits significant revisions. However, substrate concentration has a consistent and substantial effect on mass transfer. Increasing substrate concentration diminishes mass transfer limitations driven by diffusional restrictions depicted in Fig. 6(a–d), for different degree of conversions $X = 0, 0.9$ respectively. The Thiele modulus describes the effects, with higher values indicating greater mass transfer limitations. Inhibition decreases product accumulation within the catalyst, thereby reducing the reaction rate and substrate consumption in Fig. 7 (a–d) and Fig. 8(a–d), for various degree of conversions $X = 0, 0.9$ respectively.

The proposed MADM solution, which involves truncating the Taylor expansion, exhibits divergence at certain β_{b0} and Φ_1 combinations, leading to negative substrate concentrations within the catalyst. The error affects the effectiveness factor calculations. Negative values of the effectiveness factor are obtained under conditions of significant diffusional limitations. This is due to the negative substrate concentration values obtained in the invalid solution approximation zones. The validity range of the solution is

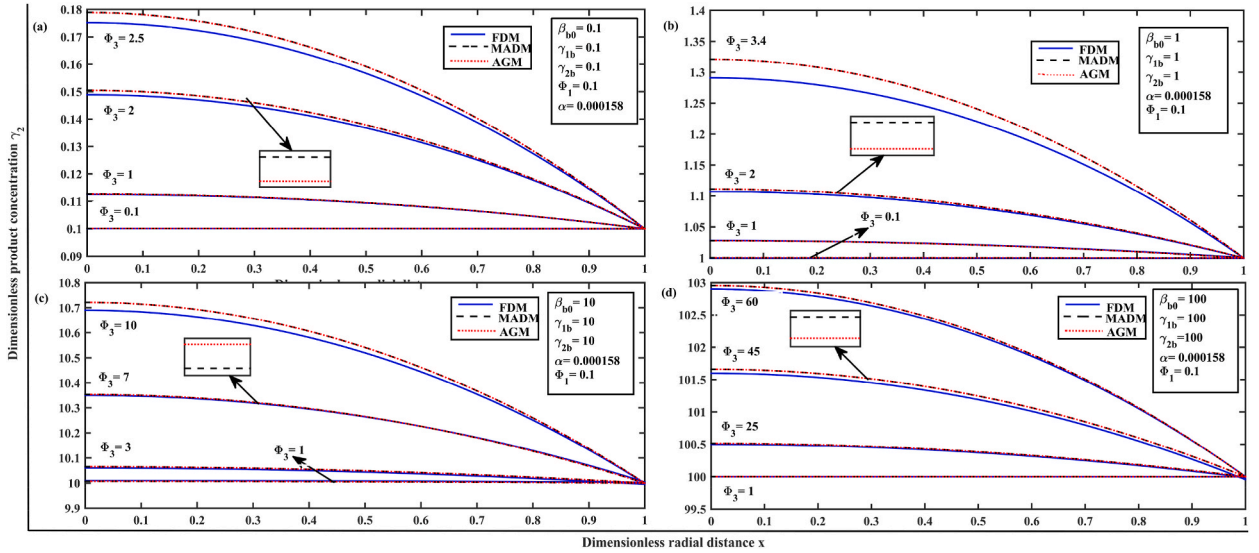

Fig. 4. Comparison of dimensionless product concentration γ_2 versus dimensionless radial distance x with numerical simulation results (FDM) for various diffusional restrictions and different initial bulk product concentration γ_{2b} (a) 0.1 (b) 1 (c) 10 and (d) 100 using Eq. (14), (21) and (24).

reliant upon the kinetic mechanism, and is denoted by Eq. (31). Fig. 9(a and b), depicts the restricted area (white), wherein the solutions for the mechanisms yield positive values for all possible combinations of β_{b0} and Φ_1. Invalid solutions are typically observed when diffusional restrictions are significant. Fig. 9(a and b), displays the acceptable and unacceptable regions with β_{b0} and Φ_1 combinations at different degree of conversion $X = 0, 0.9$ respectively. In cases of competitive inhibition, an increase in conversion and product concentration results in a decrease in the validity zone of the solution. The observed effect is a result of elevated diffusional limitations caused by increased product inhibition.

To analyze the precision of the analytical approach utilizing a finite amount of terms, the system of differential equations ((12)–(14)) was also solved numerically by the PDE-solving function, pdepe (finite difference method), FDM [40]. Matlab/Scilab coding [46] is also mentioned in Appendix E. To show the efficiency of our proposed solution, we compared our two analytical results, the AGM equations (20) and (21) and the MADM equations (22)–(24) with the numerical simulation of equations (12)–(14). In addition, we have provided the tables for error percentage on plots in Table 1(a - b) and 2 (a - b), which demonstrate a satisfactory level of agreement. In all the cases, the concentration of substrate and products reflects average relative errors of (0.0007 % in AGM, 0.00067

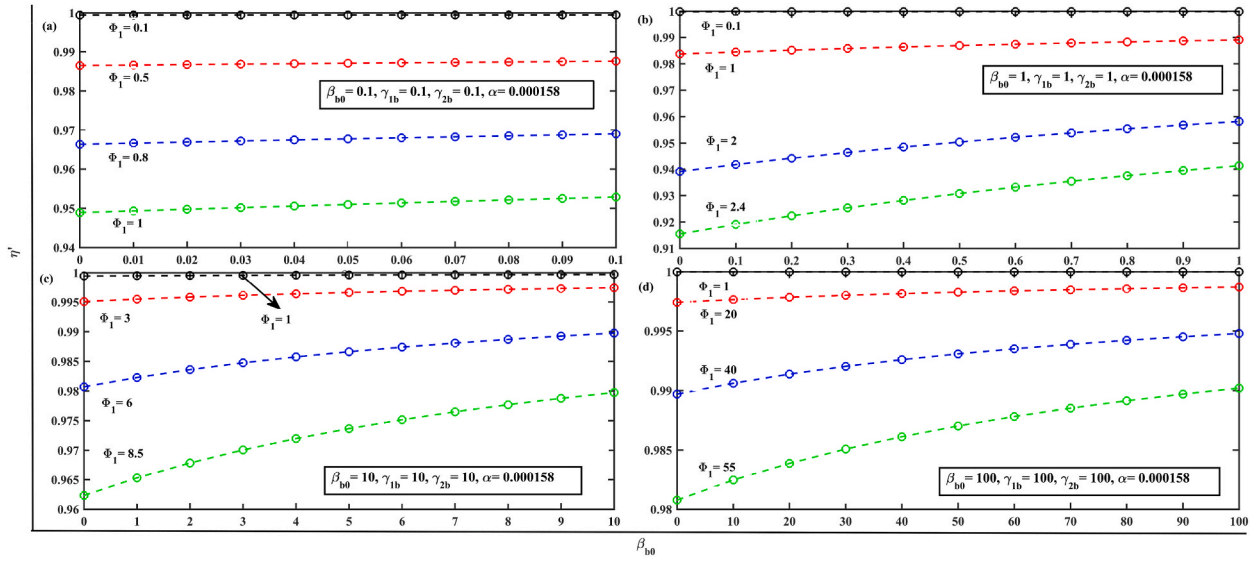

Fig. 5. Dynamics of effectiveness factor during batch reactor operation η' **versus dimensionless substrate concentration β_{b0} with different diffusional restrictions Φ_1 for different initial bulk substrate concentration β_{b0} (a) 0.1 (b) 1 (c) 10 and (d) 100 using (AGM, Eq. (35)).**

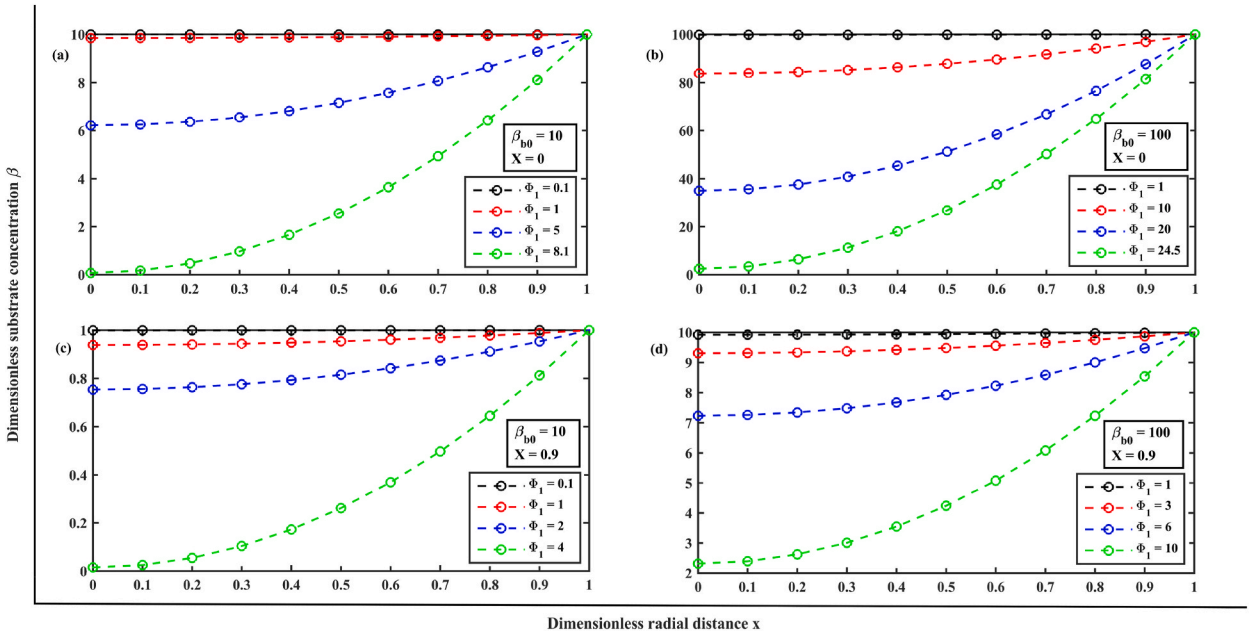

Fig. 6. Dynamics of dimensionless substrate concentration β **versus dimensionless radial distance** x **with different diffusional restrictions** Φ_1 **for initial bulk substrate concentration (a)** $\beta_{b0} = 10$, **when degree of conversions** $X = 0$, **(b)** $\beta_{b0} = 100$, **when** $X = 0$, **(c)** $\beta_{b0} = 10$, **when** $X = 0.9$, **and (d)** $\beta_{b0} = 100$, **when** $X = 0.9$, **using the Eq. (27) and** $\alpha = 0.000158$, $K = 0.13$, $K_1 = 1.82$, $K_2 = 48$.

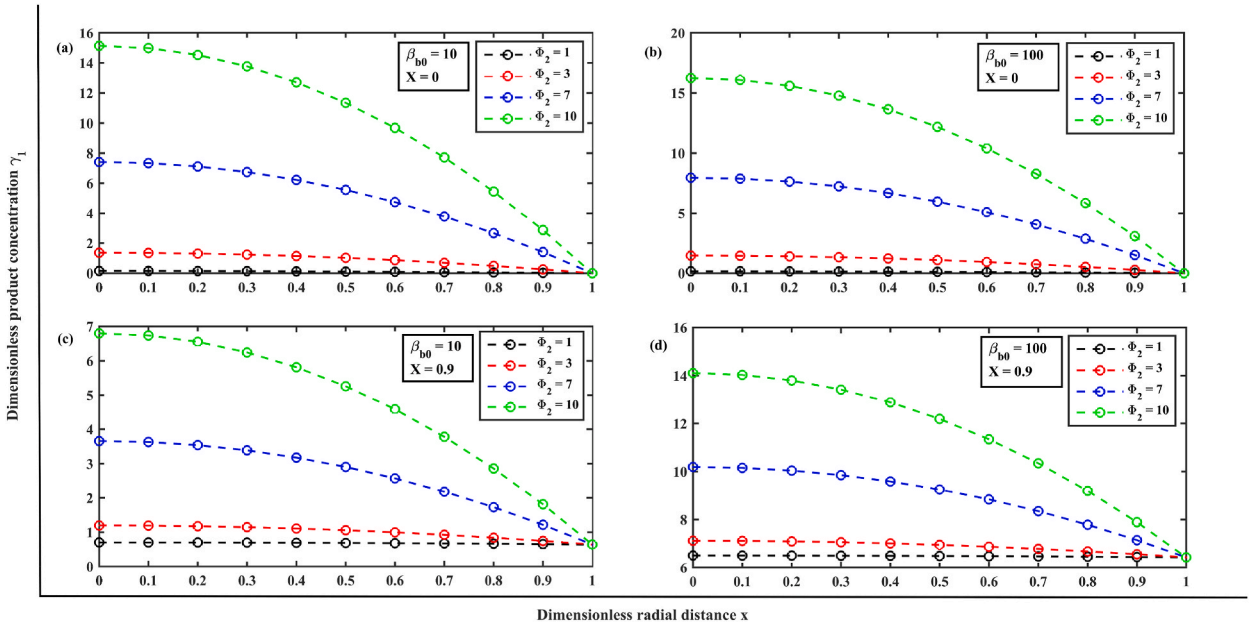

Fig. 7. Dynamics of dimensionless product concentrations γ_1 **versus dimensionless radial distance** x **with different diffusional restrictions** Φ_2 **for initial bulk substrate concentration (a)** $\beta_{b0} = 10$, **when degree of conversions** $X = 0$, **(b)** $\beta_{b0} = 100$, **when** $X = 0$, **(c)** $\beta_{b0} = 10$, **when** $X = 0.9$, **and (d)** $\beta_{b0} = 100$, **when** $X = 0.9$, **using the Eq. (28) and** $\alpha = 0.000158$, $K = 0.13$, $K_1 = 1.82$, $K_2 = 48$.

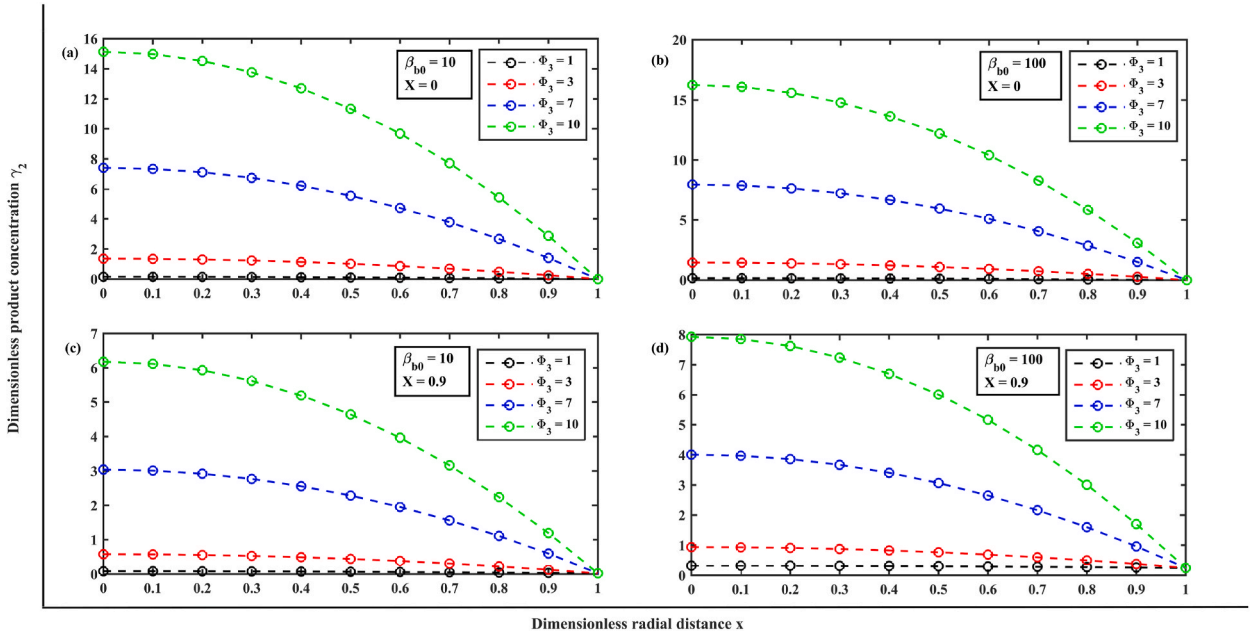

Fig. 8. Dynamics of dimensionless product concentration γ_2 **versus dimensionless radial distance** x **with different diffusional restrictions** Φ_3 **for initial bulk substrate concentration (a)** $\beta_{b0} = 10$, **when degree of conversions** $X = 0$, **(b)** $\beta_{b0} = 100$, **when** $X = 0$, **(c)** $\beta_{b0} = 10$, **when** $X = 0.9$, **and (d)** $\beta_{b0} = 100$, **when** $X = 0.9$, **using the Eq. (29) and** $\alpha = 0.000158$, $K = 0.13$, $K_1 = 1.82$, $K_2 = 48$.

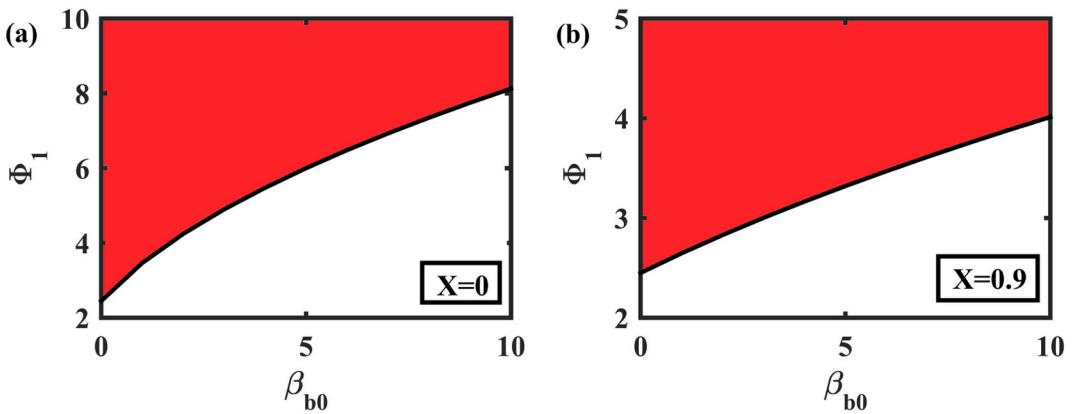

Fig. 9. Limitation of the proposed solution using (MADM, Eq. (31)) at different degree of conversions X **(a) 0 and (b) 0.9 where valid region (depicts the white zone) and invalid region (depicts the red zone).**

% in MADM) and (0.0516 % in AGM, 0.0002 % in MADM) respectively, as determined by comparing our analytical results with numerical results. It can be inferred from our analysis that there is no significant difference between numerical and analytical solutions across a range of Thiele modulus values $\Phi_i; i = 1, 2, 3$. The AGM solution provides a closed-form analytical solution, despite the MADM method is more comprehensive. The AGM method exhibits greater efficiency than the MADM method, as evidenced by the analysis of the graphs and tables. The MADM method is quite diverse compared to the AGM method for establishing the mean integrated effectiveness factor.

6. Conclusion

The steady state condition of immobilized enzymes (penicillin G acylase) under internal diffusional restrictions is analyzed over a wide range of parameters using a mathematical model. This paper outlines the derivation for substrate and product concentrations using two approximate semi-analytical approaches, using AGM and the MADM. The effect of the parameters on the concentration profiles and Thiele moduli's impact pertaining to the substrate and product concentrations were discussed. Our analytical solutions were compared to numerical simulations, and a satisfactory level of agreement was observed. This study analyzed the limitations of a proposed strategy at varying degrees of conversion, considering both valid and invalid regions, and identified suitable combinations of initial bulk concentration and Thiele modulus that result in dependable concentration profiles within the catalyst and effectiveness factor. The analytical expressions derived in this study enable quick computation of the impact of diffusional limits on concentration profiles within the catalyst particle and effectiveness factor values. Based on the aforementioned, it can be concluded that the solution obtained by the AGM method is better for computation. Thus, this tool plays an important role in the design and effectiveness of immobilized enzyme reactors, particularly in determining the optimal radius of catalyst particles.

Data availability statement

We have added the "Supplementary Material" in the "Attach file" section.

CRediT authorship contribution statement

L. Niyaz Ahmed: Writing – review & editing, Writing – original draft, Software, Methodology, Investigation, Formal analysis, Conceptualization. **Praveen T:** Writing – review & editing, Writing – original draft, Supervision, Software, Resources, Methodology, Investigation, Formal analysis, Conceptualization.

Declaration of competing interest

The authors declare that they have no known competing financial interests or personal relationships that could have appeared to influence the work reported in this paper.

Appendix A. Supplementary data

Supplementary data to this article can be found online at https://doi.org/10.1016/j.heliyon.2023.e21998.

References

[1] Shweta Pandey, Shyamal K. Goswami, Buddhi Prakash Jain, Protocols in Biochemistry and Clinical Biochemistry, Academic Press, 2020.
[2] S.P. Dwivedi, Fundamentals Of Fermentation Technology, 2023.
[3] Roger A. Sheldon, Sander van Pelt, Enzyme immobilisation in biocatalysis: why, what and how, Chem. Soc. Rev. 42 (15) (2013) 6223–6235.
[4] Roger A. Sheldon, Enzyme immobilization: the quest for optimum performance, Adv. Synth. Catal. 349 (8-9) (2007) 1289–1307.
[5] Mozhgan Razzaghi, Homaei Ahmad, Fabio Vianello, Azad Taha, Tanvi Sharma, Ashok Kumar Nadda, Roberto Stevanato, Muhammad Bilal, Hafiz MN. Iqbal, Industrial applications of immobilized nano-biocatalysts, Bioproc. Biosyst. Eng. (2022) 1–20.
[6] Ahmad Homaei, Immobilization of Penaeus merguiensis alkaline phosphatase on gold nanorods for heavy metal detection, Ecotoxicol. Environ. Saf. 136 (2017) 1–7.
[7] Neda Ranjbari, Mozhgan Razzaghi, Roberto Fernandez-Lafuente, Fozieh Shojaei, Mohammad Satari, Homaei Ahmad, Improved features of a highly stable protease from Penaeus vannamei by immobilization on glutaraldehyde activated graphene oxide nanosheets, Int. J. Biol. Macromol. 130 (2019) 564–572.
[8] Sara Bahri, Homaei Ahmad, Elaheh Mosaddegh, Zinc sulfide-chitosan hybrid nanoparticles as a robust surface for immobilization of Sillago sihama α-amylase, Colloids Surf. B Biointerfaces 218 (2022), 112754.
[9] A. Homaei, Enzyme immobilization and its application in the food industry, Advances in food biotechnology (2015) 145–164.
[10] Edward Lansing Cussler, Diffusion: Mass Transfer in Fluid Systems, Cambridge university press, 2009.
[11] Robert Holt, "Biocatalysis: Fundamentals and Applications by Andreas S. Bommarius and Bettina Riebel, 600 pp.£ 90/135 euro. ISBN 3-527-30344-8." (2004), Wiley-VCH, Weinheim, 2004, p. 814, 814.
[12] Rutherford Aris, The Mathematical Theory of Diffusion and Reaction in Permeable Catalysts: the Theory of the Steady State, vol. 1, Clarendon Press, 1975.
[13] Andrés Illanes, Lorena Wilson, 6.2 synthesis of β-lactam antibiotics with penicillin acylases, Enzyme Biocatalysis (2008) 273.
[14] Margreth A. Wegman, Michiel Ha Janssen, Fred van Rantwijk, Roger A. Sheldon, Towards biocatalytic synthesis of β-lactam antibiotics, Adv. Synth. Catal. 343 (6-7) (2001) 559–576.
[15] M. Arroyo, I. De la Mata, C. Acebal, M. Pilar Castillon, Biotechnological applications of penicillin acylases: state-of-the-art, Appl. Microbiol. Biotechnol. 60 (2003) 507–514.
[16] A. Illanes, L. Wilson, C. Altamirano, Z. Cabrera, L. Alvarez, C. Aguirre, Production of cephalexin in organic medium at high substrate concentrations with CLEA of penicillin acylase and PGA-450, Enzym. Microb. Technol. 40 (2) (2007) 195–203.
[17] Pedro Valencia, Sebastián Flores, Lorena Wilson, Andrés Illanes, Effect of particle size distribution on the simulation of immobilized enzyme reactor performance, Biochem. Eng. J. 49 (2) (2010) 256–263.
[18] Juan I. Ramos, Exponential methods for one-dimensional reaction–diffusion equations, Appl. Math. Comput. 170 (1) (2005) 380–398.
[19] Davoodi Ganji, Salim Karimpour, Seyedreza Ganji, Approximate analytical solutions to nonlinear oscillations of non-natural systems using he's energy balance method, Prog. Electromagn. Res. M 5 (2008) 43–54.
[20] R.S. Kaushal, Ranjit Kumar, and Awadhesh Prasad. "On the exact solutions of nonlinear diffusion-reaction equations with quadratic and cubic nonlinearities.", Pramana 67 (2006) 249–256.

[21] M.S.H. Chowdhury, I. Hashim, Analytical solution for Cauchy reaction-diffusion problems by homotopy perturbation method, Sains Malays. 39 (3) (2010) 495–504.
[22] Mohammadreza Akbari, Alireza Ahmadi, Davood Domairry Ganji, Nonlinear Dynamic in Engineering by Akbari-Ganji's Method, Xlibris Corporation, 2015.
[23] T. Praveen, Pedro Valencia, L. Rajendran, Theoretical analysis of intrinsic reaction kinetics and the behavior of immobilized enzymes system for steady-state conditions, Biochem. Eng. J. 91 (2014) 129–139.
[24] P. Valencia, S. Flores, L. Wilson, A. Illanes, Effect of internal diffusional restrictions on the hydrolysis of penicillin G: reactor performance and specific productivity of 6-APA with immobilized penicillin acylase, Appl. Biochem. Biotechnol. 165 (2011) 426–441.
[25] Jean-Marc Engasser, A fast evaluation of diffusion effects on bound enzyme activity, Biochim. Biophys. Acta Enzymol. 526 (2) (1978) 301–310.
[26] Peter Grunwald, Determination of effective diffusion coefficients—an important parameters for the efficiency of immobilized biocatalysts, Biochem. Educ. 17 (2) (1989) 99–102.
[27] R. Senthamarai, T.N. Saibavani, Substrate mass transfer: analytical approach for immobilized enzyme reactions, J. Phys. Conf. 1000 (1) (2018), 012146. IOP Publishing.
[28] Vincent PonRani, Michael Raj Margret, Lakshmanan Rajendran, Eswaran Raju, Analytical expression of the substrate concentration in different part of particles with immobilized enzyme and substrate inhibition kinetics, Analytical and Bioanalytical Electrochemistry 3 (2011) 507–520.
[29] Salim Hamrelaine, Mohamed Kezzar, Mohamed Rafik Sari, Mohamed R. Eid, Analytical investigation of hydromagnetic ferro-nanofluid flowing via rotating convergent/divergent channels, The European Physical Journal Plus 137 (11) (2022) 1291.
[30] Chahra M. Ayeche, Mohamed Kezzar, Mohamed R. Sari, Mohamed R. Eid, Analytical ADM study of time-dependent hydromagnetic flow of biofluid over a wedge, Indian J. Phys. 95 (12) (2021) 2769–2784.
[31] Sihem Gherieb, Mohamed Kezzar, Mohamed Rafik Sari, Analytical and numerical solutions of heat and mass transfer of boundary layer flow in the presence of a transverse magnetic field, Heat Transfer 49 (3) (2020) 1129–1148.
[32] Kezzar Mohamed, Tabet Ismail, Nafir Nourreddine, Sari Mohamed Rafik, Analytical study of nano-bioconvective flow in a horizontal channel using Adomian decomposition method, J. Comput. Appl. Res. Mech. Eng. 9 (2) (2020) 245–258.
[33] Kezzar. M. O. H. A. M. E. D, Sari Mohamed Rafik, , R. A. C. H. I. D. Adjabi, Ammar Haiahem, A modified decomposition method for solving nonlinear problem of flow in converging-diverging channel, J. Eng. Sci. Technol. 10 (2015) 1035–1053.
[34] Rathinasamy Angel Joy, Athimoolam Meena, Shunmugham Loghambal, Lakshmanan Rajendran, A two-parameter mathematical model for immobilized enzymes and Homotopy analysis method, Nat. Sci. 3 (7) (2011) 556.
[35] Sihem Gherieb, Mohamed Kezzar, Abdelaziz Nehal, Mohamed Rafik Sari, A new improved generalized decomposition method (improved-GDM) for hydromagnetic boundary layer flow, Int. J. Numer. Methods Heat Fluid Flow 30 (10) (2020) 4607–4628.
[36] Wassila Fenizri, Mohamed Kezzar, Mohamed R. Sari, Ismail Tabet, Mohamed R. Eid, New modified decomposition method (DRMA) for solving MHD viscoelastic fluid flow: comparative study, Int. J. Ambient Energy 43 (1) (2022) 3686–3694.
[37] Mounir Gahgah, Mohamed R. Sari, Mohamed Kezzar, Mohamed R. Eid, Duan–Rach modified Adomian decomposition method (DRMA) for viscoelastic fluid flow between nonparallel plane walls, The European Physical Journal Plus 135 (2) (2020) 250.
[38] Mohamed Kezzar, Ismail Tabet, Mohamed R. Eid, A new analytical solution of longitudinal fin with variable heat generation and thermal conductivity using DRA, The European Physical Journal Plus 135 (1) (2020) 1–15.
[39] P.A. Ramachandran, Application of the boundary element method to non-linear diffusion with reaction problems, Int. J. Numer. Methods Eng. 29 (5) (1990) 1021–1031.
[40] Evelina Gaidamauskaitė, Romas Baronas, A comparison of finite difference schemes for computational modelling of biosensors, Nonlinear Anal. Model Control 12 (3) (2007) 359–369.
[41] Noya Loew, Takashi Ofuji, Isao Shitanda, Yoshinao Hoshi, Yuki Kitazumi, Kenji Kano, Masayuki Itagaki, Cyclic voltammetry and electrochemical impedance simulations of the mediator-type enzyme electrode reaction using finite element method, Electrochim. Acta 367 (2021), 137483.
[42] M.M. Hosseini, M. Jafari, A note on the use of Adomian decomposition method for high-order and system of nonlinear differential equations, Commun. Nonlinear Sci. Numer. Simul. 14 (2009) 1952–1957.
[43] J. Biazar, A.R. Amirtaimoori, An analytic approximation to the solution of heat equation by Adomian decomposition method and restrictions of the method, Appl. Math. Comput. 171 (2005) 738–745.
[44] S. Saha Ray, R.K. Bera, An approximate solution of a nonlinear fractional differential equation by Adomian decomposition method, Appl. Math. Comput. 167 (2005) 561–571.
[45] M. Moo-Young, Takeshi Kobayashi, Effectiveness factors for immobilized-enzyme reactions, Can. J. Chem. Eng. 50 (2) (1972) 162–167.
[46] MATLAB 6.1, The Mathworks Inc. Natick, MA, 2000.

List of Symbols. Nomenclature

D_e: effective diffusion coefficient of substrate ($cm^2\ s^{-1}$)
D_{e1}: effective diffusion coefficient of PAA ($cm^2\ s^{-1}$)
D_{e2}: effective diffusion coefficient of 6-APA ($cm^2\ s^{-1}$)
E: enzyme concentration inside catalyst ($mol\ cm^{-3}$)
k: reaction rate constant ($mol\ cm^{-3}\ s^{-1}$)
K_1: product inhibition constant for PAA ($mol\ cm^{-3}$)
K_2: product inhibition constant for 6-APA ($mol\ cm^{-3}$)
K_S: Pen G substrate inhibition constant ($mol\ cm^{-3}$)
K: substrate Michaelis constant (Pen G model is present) ($mol\ cm^{-3}$)
S: substrate concentration inside biocatalyst ($mol\ cm^{-3}$)
P_1: concentration of product PAA ($mol\ cm^{-3}$)
P_2: concentration of product 6-APA ($mol\ cm^{-3}$)
S_b: bulk concentration of a substrate ($mol\ cm^{-3}\ s^{-1}$)
S_{b0}: initial bulk concentration of a substrate
P_i: concentration of products i ($mol\ cm^{-3}$)
P_{bi}: bulk concentration of a products i ($mol\ cm^{-3}\ s^{-1}$)
P_{b0}: initial bulk concentration of a product
r: variable radius inside the biocatalyst particle (cm)
R: biocatalyst particle radius (cm)
t: reaction time (s)
X: degree of conversion

Dimensionless parameters (Greek symbols)

$\beta = \frac{S}{K}$: dimensionless concentration of a substrate
$\beta_b = \frac{S_b}{K}$: dimensionless concentration of a substrate outside the support
β_{b0}: dimensionless initial bulk concentration of a substrate

$\gamma_i = \frac{P_i}{K_i}, i = 1, 2$: dimensionless concentration of the products i
$\gamma_{ib} = \frac{P_i}{K_i}, i = 1, 2$: dimensionless concentration of the products outside the support i
$x = \frac{r}{R}$: dimensionless radial distance
$\alpha = \frac{K}{K_s}$: dimensionless inhibition degree
$\Phi_1 = R\sqrt{\frac{k \cdot E}{K \cdot D_e}}$: Thiele modulus for substrate
$\Phi_{i+1} = R\sqrt{\frac{k \cdot E}{K_i \cdot D_{ei}}}, i = 1, 2$: Thiele modulus for products i
η: local effectiveness factor
$\bar{\eta}$: mean integrated effectiveness factor

Abbreviations

AGM: Akbari-Ganji's method
MADM: Modified Adomian decomposition method
FDM: Finite difference method
Pen G: Penicillin G
PAA: Phenyl acetic acid
6-APA: 6-aminopenicillanic acid